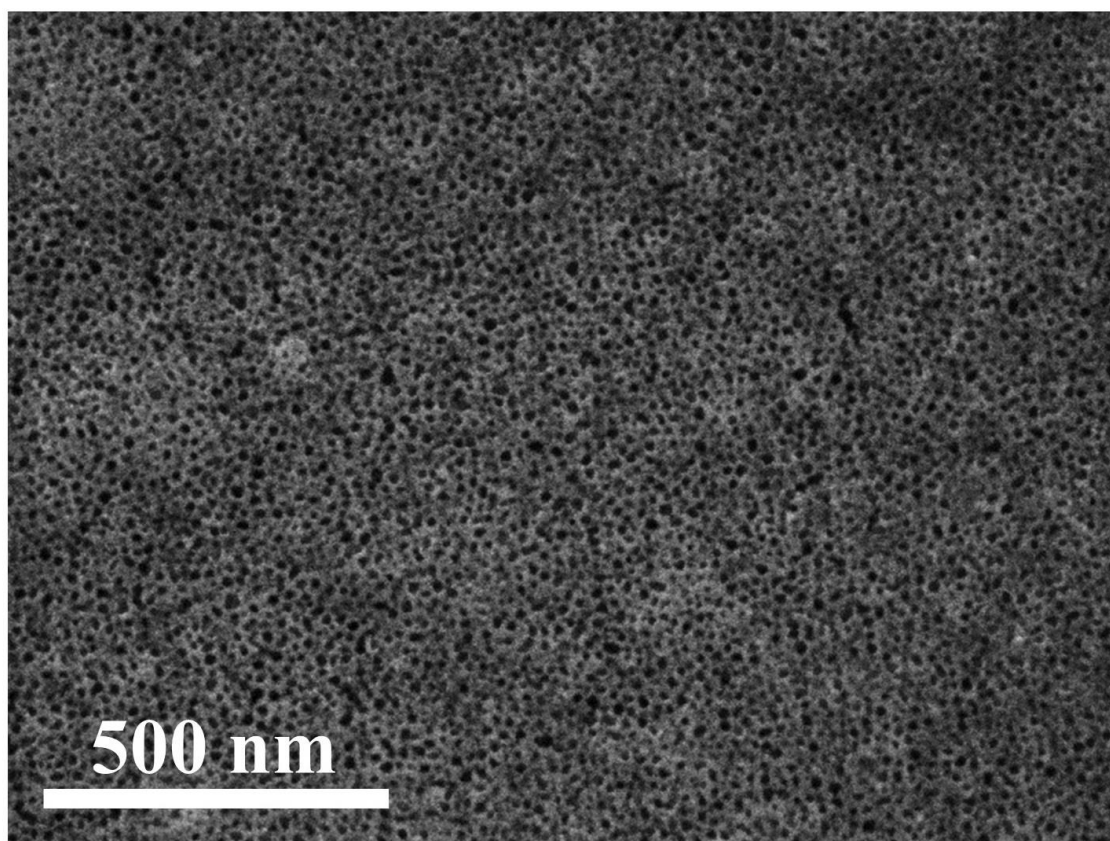
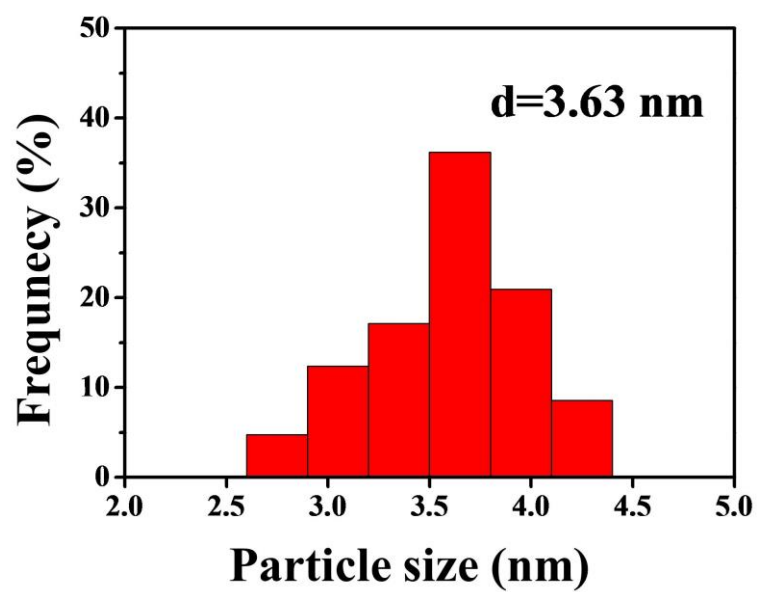


**Fig. S1** SEM image of the mPtRu-NF.



**Fig. S2** SEM image of the mPtRu-NF.



**Fig. S3** The particle size distribution histogram of PtRu nanoparticles.

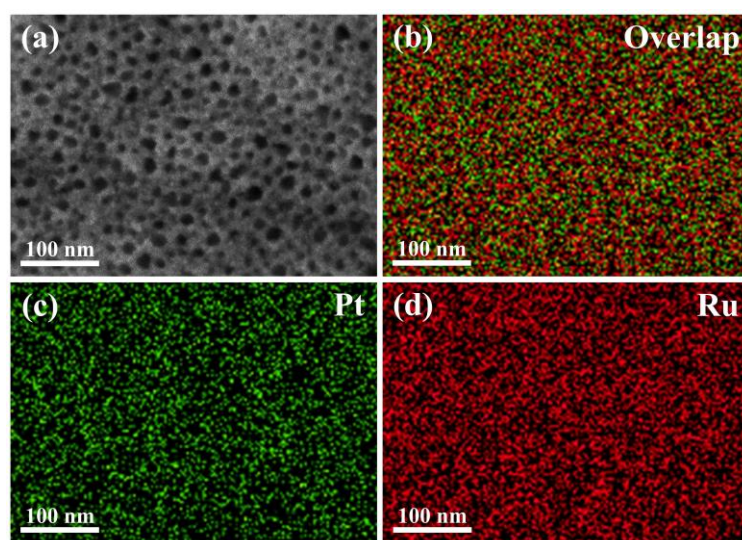


**Fig. S4** (a) SEM image and (b, c and d) elemental mapping images of the mPtRu-NF.

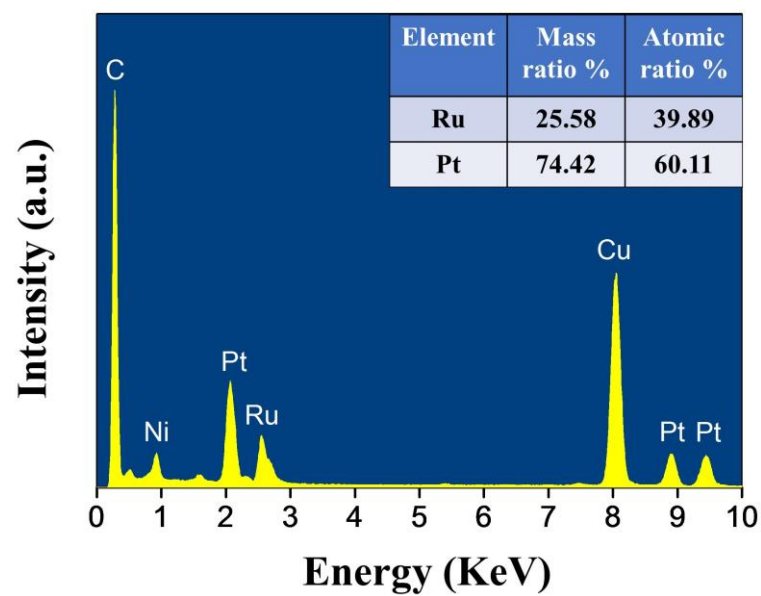


**Fig. S5** TEM-EDX image of the mPtRu-NF.

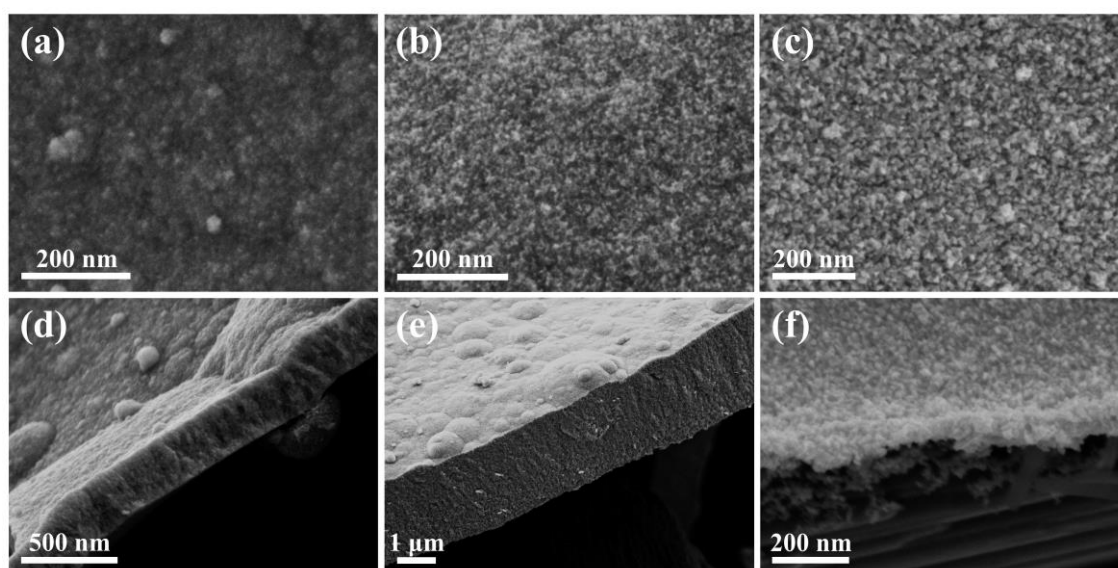


**Fig. S6** SEM images of the top-surface and cross-section views of the PtRu-NF prepared by replacing F127 with (a, d) Brij 58, (b, e) PVP, and (c, f) without surfactants, respectively, under the typical conditions used for the typical synthesis.

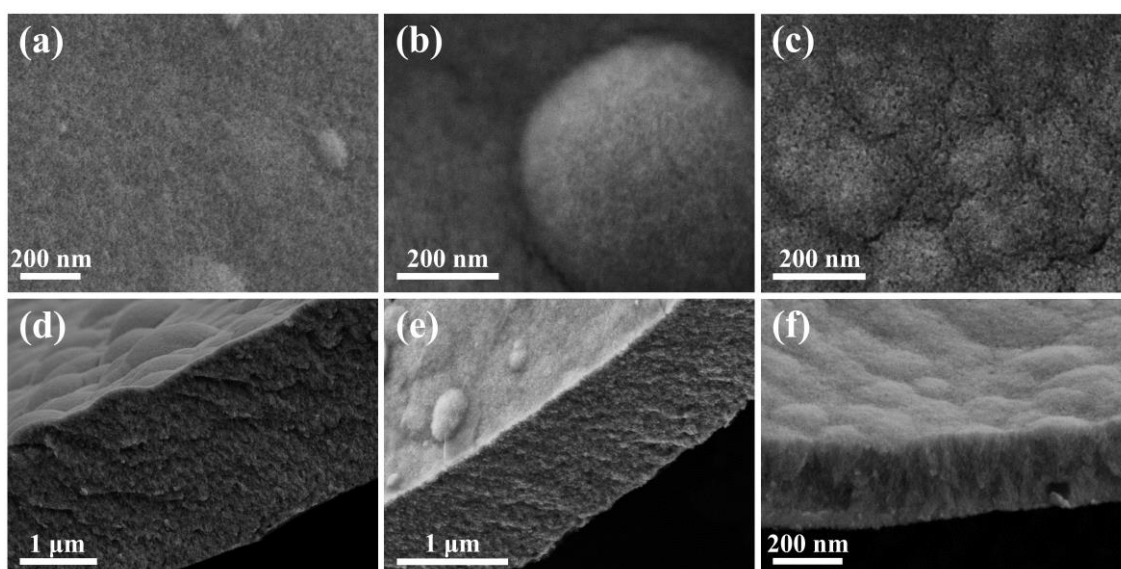


**Fig. S7** SEM images of the top-surface and cross-section views of the samples prepared under the typical conditions with (a, d) 0  $\mu\text{L}$ , (b, e) 5  $\mu\text{L}$  and (c, f) 125  $\mu\text{L}$  HCl (6 M), respectively.

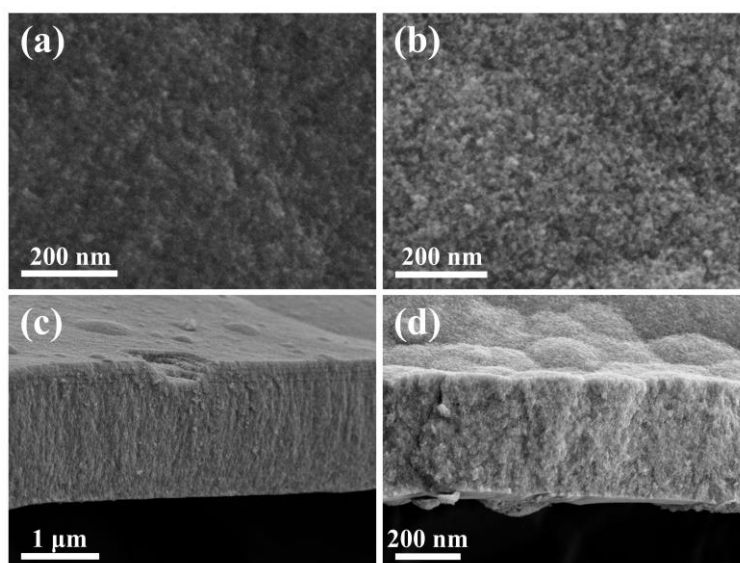


**Fig. S8** SEM images of the top-surface and cross-section views of the samples prepared by replacing HCl with (a, c)  $\text{HNO}_3$  and (b, d)  $\text{H}_2\text{SO}_4$ , respectively, under the typical conditions used for the typical synthesis.

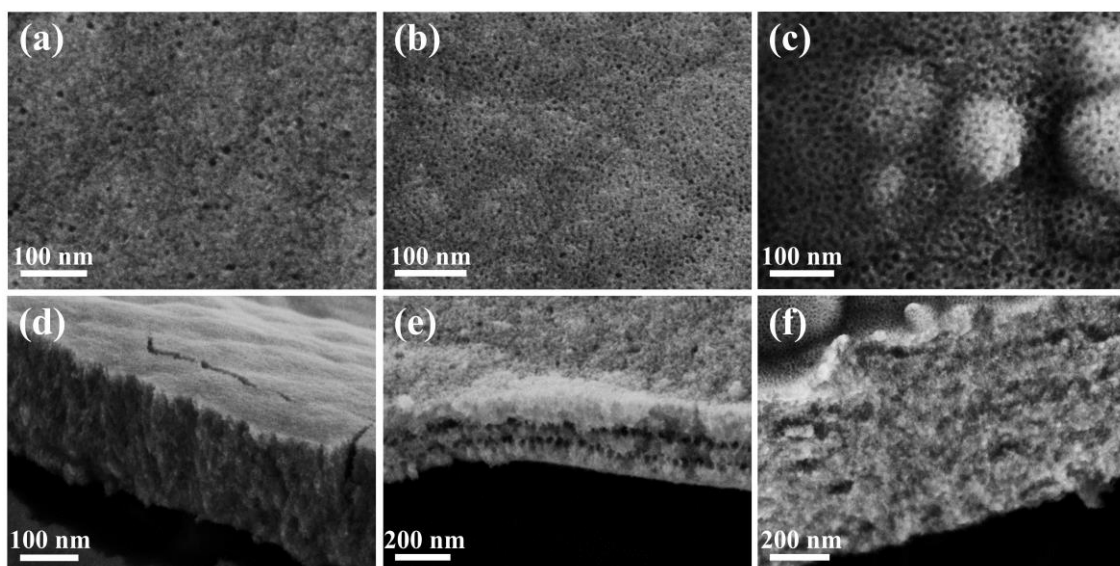


**Fig. S9** SEM images of the top-surface and cross-section views of the samples prepared under the typical conditions for (a, d) 3 h, (b, e) 6 h and (c, f) 24 h, respectively.

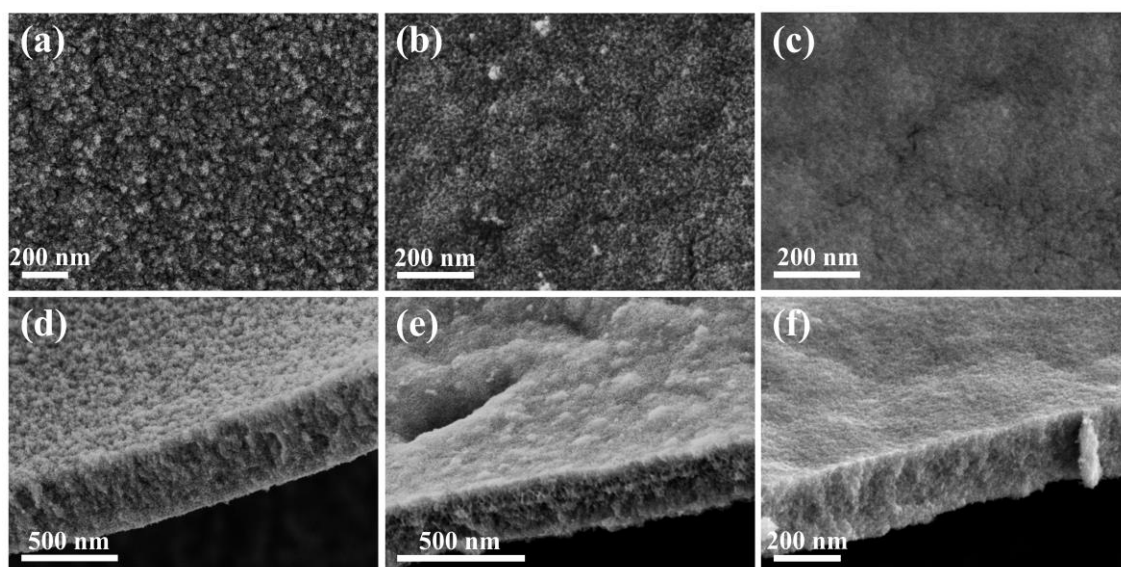


**Fig. S10** SEM images of the top-surface and cross-section views of the samples prepared with different amounts of the metallic precursors. The added amounts of metallic precursors,  $\text{K}_2\text{PtCl}_4$  and  $\text{RuCl}_3$  are (a, d) 3.0 mL and 0 mL (Pt-NF), (b, e) 2.5 mL and 0.5 mL ( $\text{Pt}_5\text{Ru}$ -NF), (c, f) 0.5 mL and 2.5 mL ( $\text{PtRu}_5$ -NF), respectively.



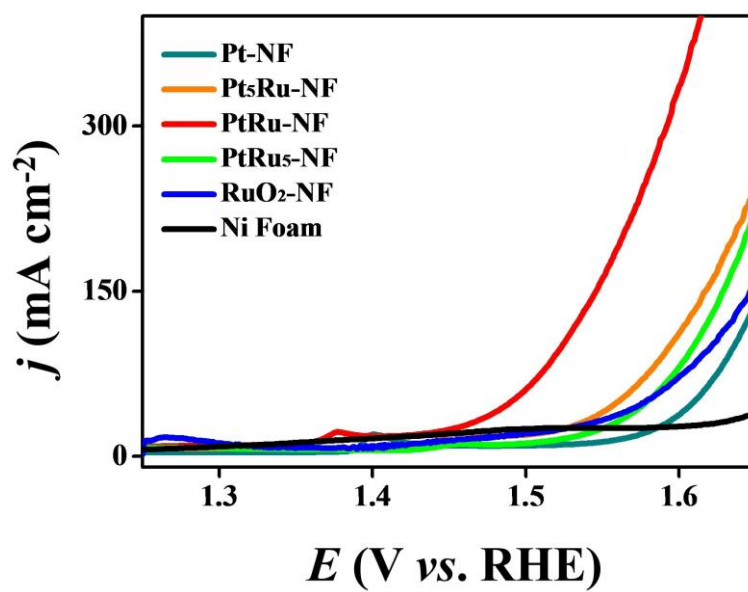


**Fig. S11** OER polarization curves. The LSVs for OER were recorded in a 1 M KOH solution at a sweep rate of 5 mV s<sup>-1</sup>.

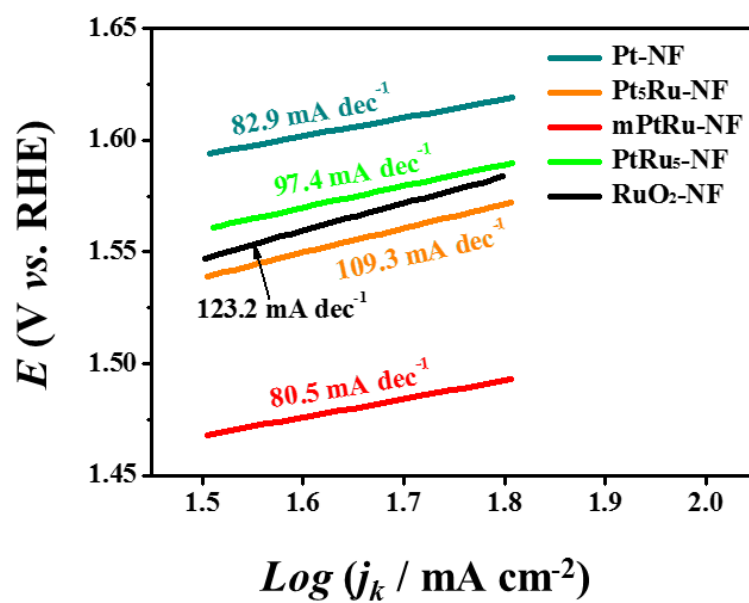


**Fig. S12** Tafel slopes of OER for the different samples.

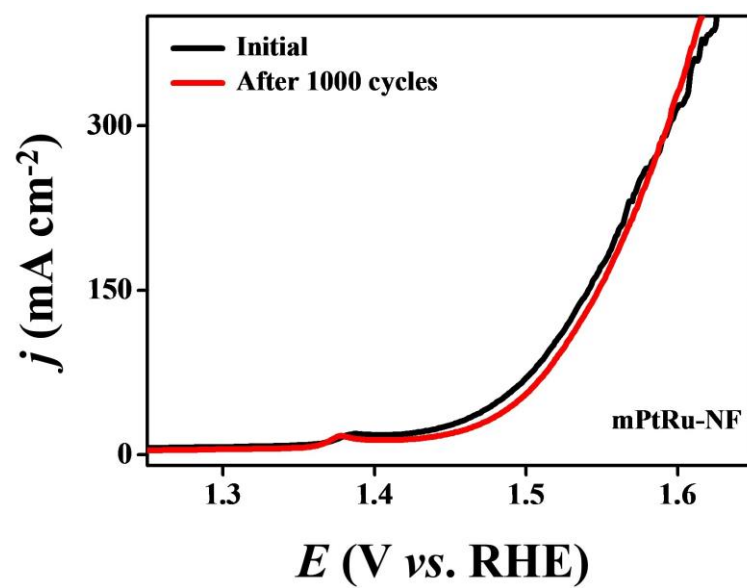


**Fig. S13** OER polarization curves before and after durability test for the mPtRu-NF.

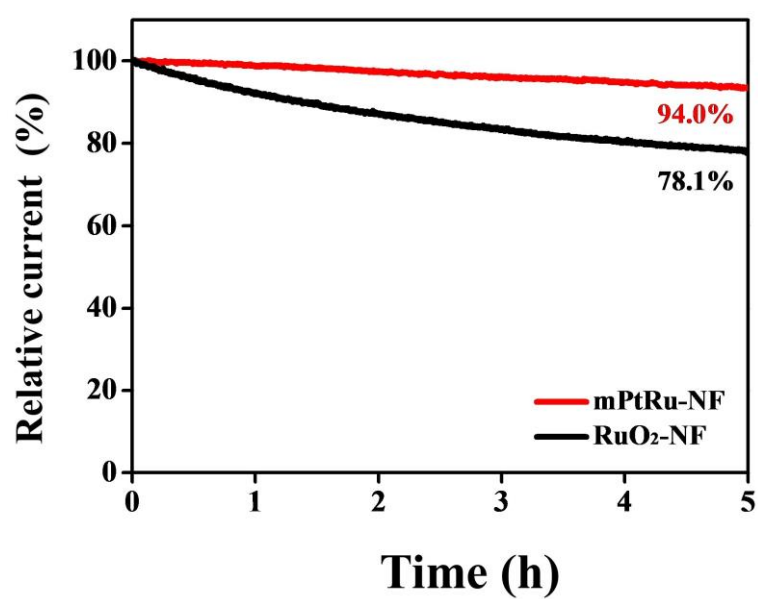


**Fig. S14** Chronoamperometric measurements of the samples tested at 1.5 V.

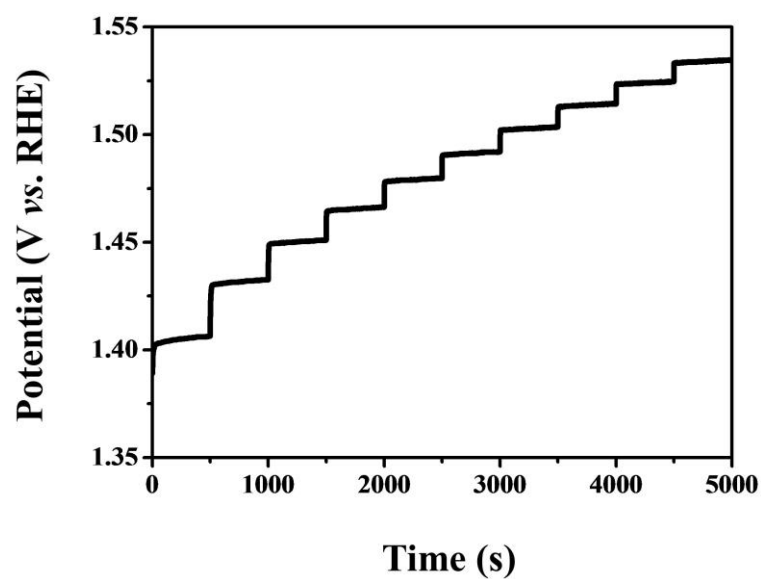


**Fig. S15** Multicurrent process of mPtRu-NF. The current density started at  $4 \text{ mA cm}^{-2}$  and ended at  $40 \text{ mA cm}^{-2}$ , using an increment of  $4 \text{ mA cm}^{-2}$  per 500 s without iR correction.

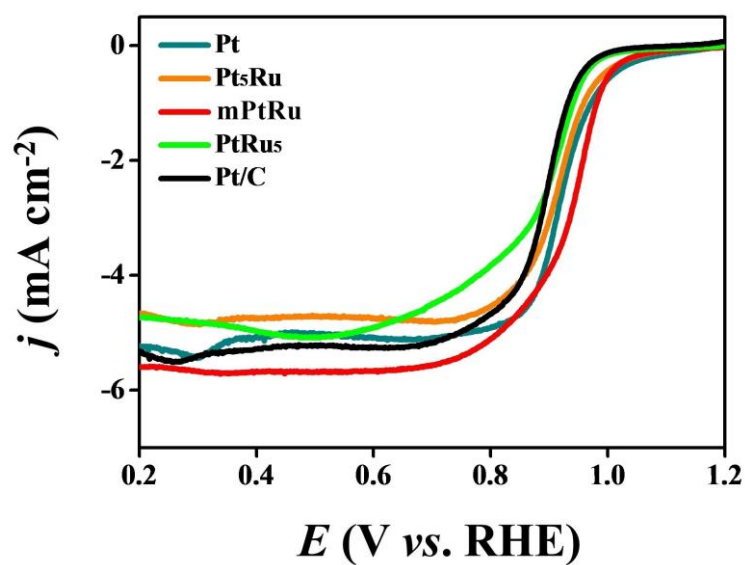


**Fig. S16** ORR polarization curves of the different samples. The LSVs for ORR were recorded in an  $\text{O}_2$ -saturated 1 M KOH solution at a sweep rate of  $5 \text{ mV s}^{-1}$  with a rotation rate of 1600 rpm.



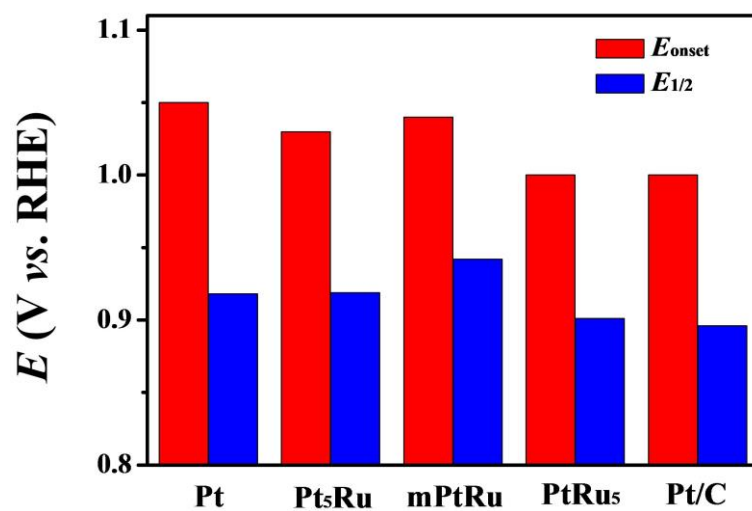


**Fig. S17** The comparisons of  $E_{\text{onset}}$  and  $E_{1/2}$  for the different samples.

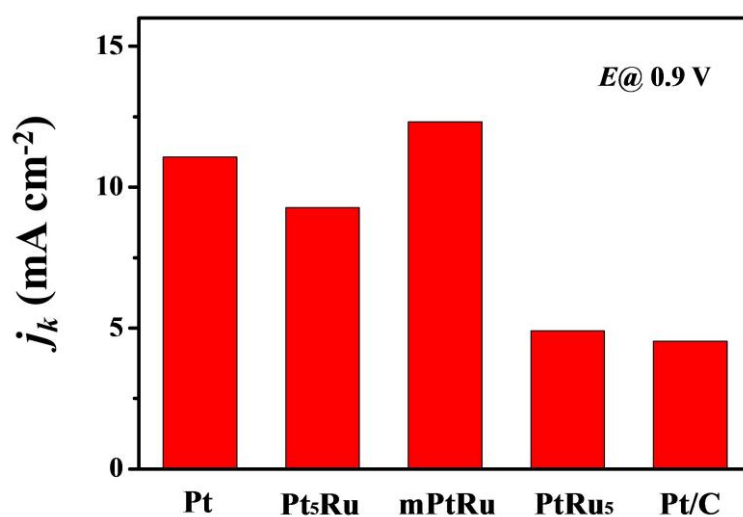


**Fig. S18** The comparison of  $j_k$  at 0.9 V for the different samples.

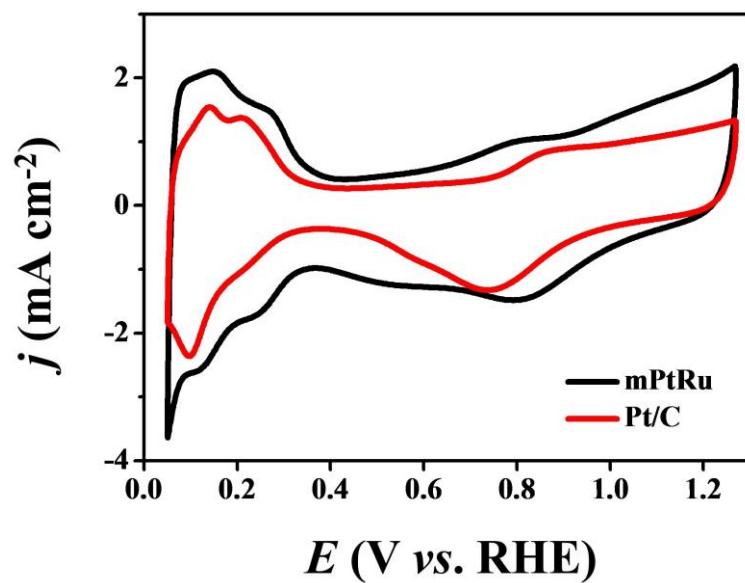


**Fig. S19** The CV curves of mPtRu and Pt/C in 0.5 M H<sub>2</sub>SO<sub>4</sub> solution at a scan rate of 50 mV s<sup>-1</sup>.

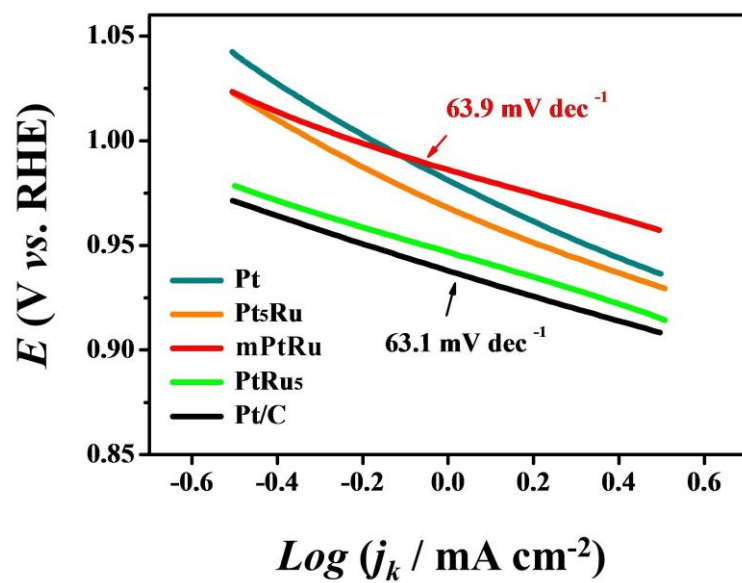


**Fig. S20** Tafel slopes of ORR for the different samples.

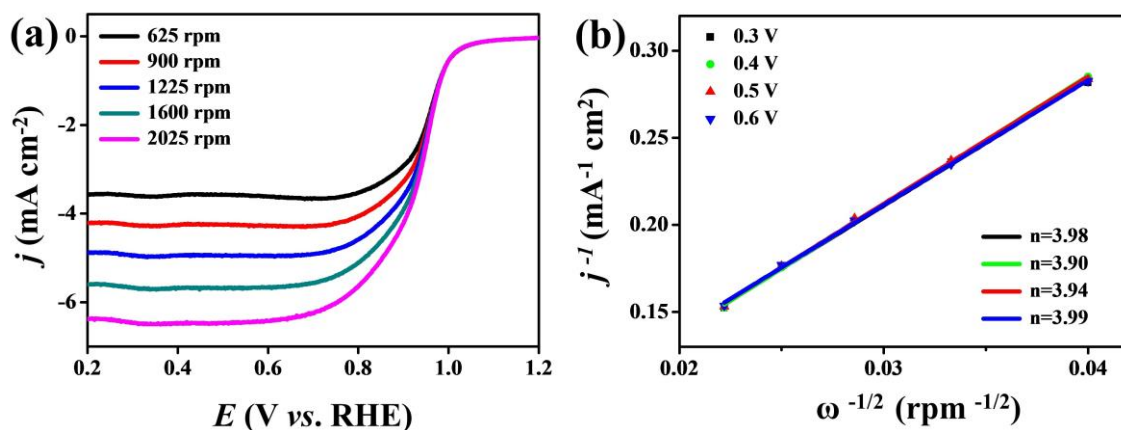


**Fig. S21** (a) ORR polarization curves of the mPtRu with different RDE rotation rates. (b) The electron transfer numbers at different potentials. The LSVs were recorded in an O<sub>2</sub>-saturated 1 M KOH solution at a sweep rate of 5 mV s<sup>-1</sup>.

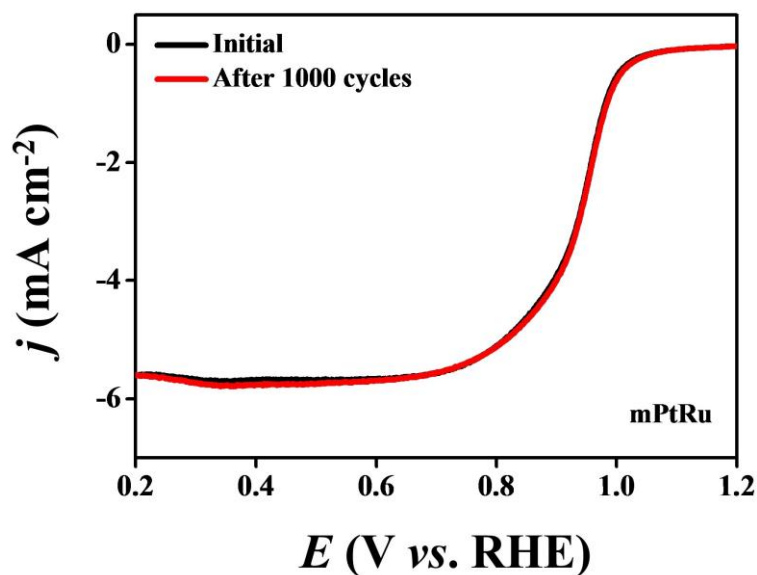


**Fig. S22** ORR polarization curves before and after durability test for the mPtRu.

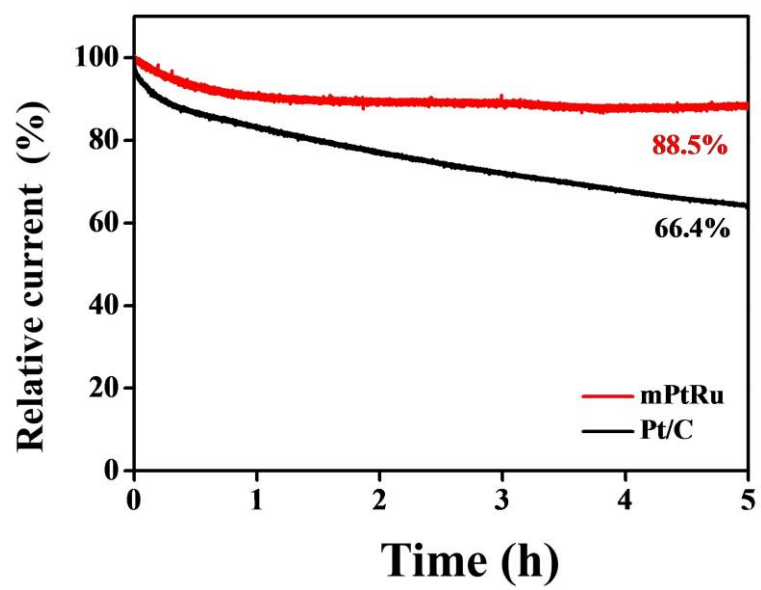


**Fig. S23** Chronoamperometric measurements of the samples tested at 0.9 V.